

Diluted mean-field spin-glass models at criticality

G Parisi^{1,2}, F Ricci-Tersenghi^{1,2} and T Rizzo³

¹ Dipartimento di Fisica, IPCF-CNR, UOS Roma, Italy

² INFN, Sezione di Roma1, Università 'La Sapienza', Piazzale Aldo Moro 2, I-00185, Rome, Italy

³ IPCF-CNR, UOS Roma, Università 'La Sapienza', Piazzale Aldo Moro 2, I-00185, Rome, Italy

E-mail: giorgio.parisi@roma1.infn.it, federico.ricci@roma1.infn.it and tomaso.rizzo@inwind.it

Received 9 January 2014

Accepted for publication 24 February 2014

Published 17 April 2014

Online at stacks.iop.org/JSTAT/2014/P04013

doi:10.1088/1742-5468/2014/04/P04013

Abstract. We present a method derived by cavity arguments to compute the spin-glass and higher order susceptibilities in diluted mean-field spin-glass models. The divergence of the spin-glass susceptibility is associated with the existence of a non-zero solution of a homogeneous linear integral equation. Higher order susceptibilities, relevant for critical dynamics through the parameter exponent λ , can be expressed at criticality as integrals involving the critical eigenvector. The numerical evaluation of the corresponding analytic expressions is discussed. The method is illustrated in the context of the de Almeida–Thouless line for a spin glass on a Bethe lattice but can be generalized straightforwardly to more complex situations.

Keywords: classical phase transitions (theory), cavity and replica method, disordered systems (theory), spin glasses (theory)

ArXiv ePrint: [1401.1729](https://arxiv.org/abs/1401.1729)

Contents

1. Introduction	2
2. Outline of the results	3
3. The equation for the critical point	5
3.1. Derivation of the equation	5
3.2. Solving the critical equation	7
3.3. The zero temperature limit	11
4. Six-point susceptibilities at criticality	14
5. Conclusions	18
Acknowledgments	18
Appendix. The SK limit at finite and zero temperature	18
References	20

1. Introduction

In disordered magnetic systems the spin-glass (SG) singularity occurs by definition for those values of the external parameters where the spin-glass susceptibility diverges [1]. The computation of this four-point correlation function in the paramagnetic phase is therefore tantamount to the location of the phase transition. Higher order (six-point) susceptibilities also play an important role because they determine the function $q(x)$ quantitatively in the replica-symmetry-breaking phase in the vicinity of the critical point [2, 3]. Recently, it has been discovered that they also determine the non-universal dynamical critical exponents quantitatively [3]–[7]. Furthermore, the same equilibrium susceptibilities are important for off-equilibrium behavior [8, 9]. In this paper we discuss the problem of the computation of these susceptibilities in mean-field spin-glass models with finite connectivity.

In mean-field spin-glass models, both fully connected and with finite connectivity, one can use the replica method in order to write down a saddle-point expression for the free energy and determine the location of the phase transition in parameter space by studying the stability of the paramagnetic solution. In fully connected models, like the Sherrington–Kirkpatrick (SK) model, the order parameter is an $n \times n$ matrix and this program can be completed both in the paramagnetic and in the spin-glass phase [1]. In the case of models with finite connectivity the replicated order parameter is a more complicated object and the computations are more difficult [10]; on the other hand, one can exploit the (local) tree-like structure of the corresponding graphs and apply the cavity method instead, thus avoiding replicas [11].

By means of the cavity method it is rather easy to obtain a self-consistent equation for the order parameter which, in the paramagnetic phase, is a probability density of the local

cavity fields. However, the self-consistent equation and its solution are perfectly regular at the SG transition and cannot be used to locate it (except in the case of strictly zero external field). Previous studies in the context of the replica method have shown that the critical point is associated instead with the solution of certain integral equations [12, 14], and the same equations have also been rederived in the context of the cavity method [13]. The cavity method derivation relies essentially on joint iterative equations for the fields and the susceptibilities, a technique that was originally developed for the study of the number of metastable states on locally tree-like models [15]. The derivation also allows one to understand the connection between the integral equations and numerical methods based on coupled systems which allowed the first quantitative description of the region of validity of the paramagnetic phase [19]. In this paper we present an alternative cavity method derivation of these integral equations and discuss their numerical solution down to zero temperature. This discussion is instrumental to the main new result that we report here, i.e. the expression, derived by cavity arguments, of the two *static* six-point susceptibilities that control the critical *dynamics*.

We will illustrate the method in the context of the de Almeida–Thouless (dAT) transition on an Ising SG defined on a random lattice with fixed connectivity, but it can be generalized straightforwardly to more complicated models in order to obtain the corresponding expressions for the same six-point susceptibilities. These extensions include, e.g., Potts spins, fluctuating connectivity and p -spin interactions. The method can also be applied to different kinds of SG phase transitions including notably some instances of discontinuous replica-symmetry-breaking transitions that display the phenomenology of structural glasses.

The plan of the paper is as follows. In section 2 we will present the results in a concise way together with their physical motivations. In section 3 we will derive the integral equation condition and we will discuss its numerical solution down to zero temperature. In section 4 we will present the derivation of the six-point susceptibilities and use it to determine them on the dAT line in the case of an SG model with connectivity $c = 4$. In section 5 we give our conclusions. In the appendix we report the detailed analysis of the high-connectivity (SK) limit.

2. Outline of the results

The spin-glass transition is characterized by the divergence of the spin-glass susceptibility χ_{SG} defined as

$$\chi_{\text{SG}} \equiv \frac{1}{N} \sum_{ij} \overline{(\langle s_i s_j \rangle - \langle s_i \rangle \langle s_j \rangle)^2} \quad (1)$$

where the angular brackets mean thermal average and the overline means disorder average. The dynamics is also critical at the phase transition. In particular, the time decay of the correlation $C(t) \equiv N^{-1} \sum_i \overline{\langle s_i(0) s_i(t) \rangle}$ is exponential in the paramagnetic phase but becomes power-law at the critical point

$$C(t) \simeq q_{\text{EA}} + \frac{c}{t^a} \quad (2)$$

where q_{EA} is the Edwards–Anderson parameter. It has been recently established [3] that the dynamical exponent a can be computed from the ratio of two *static* six-point susceptibilities; more precisely we have

$$\frac{\Gamma^2(1-a)}{\Gamma(1-2a)} = \frac{\omega_2}{\omega_1} \quad (3)$$

where $\Gamma(x)$ is the Gamma function and ω_2, ω_1 are defined as

$$\omega_1 \equiv \frac{1}{N} \sum_{ijk} \overline{\langle s_i s_j \rangle_c \langle s_j s_k \rangle_c \langle s_k s_i \rangle_c} \quad (4)$$

$$\omega_2 \equiv \frac{1}{2N} \sum_{ijk} \overline{\langle s_i s_j s_k \rangle_c^2} \quad (5)$$

where the suffix c means connected correlations [3]. Note that in the literature the so-called parameter exponent λ is often introduced, which controls a through $\Gamma^2(1-a)/\Gamma(1-2a) = \lambda$; in terms of λ equation (3) reads $\lambda = \omega_2/\omega_1$. Besides these more recent developments it is known [1, 2, 9] that the very same ratio ω_2/ω_1 is equal to the position of the breaking point in continuous RSB transitions. For instance, in the RSB phase near the dAT line (which will be studied in the following) this ratio is precisely equal to the point x where the function $q(x)$ displays a continuous part. We will provide a general method to obtain the expressions of $\chi_{\text{SG}}, \omega_1$ and ω_2 in models with finite connectivity.

In finite-connectivity models the paramagnetic phase can be described through a self-consistent equation for the distribution of the fields. In the following we specialize to the case of Ising spins in the presence of a field H interacting by means of two-body quenched couplings J_{ij} on a random regular graph, i.e. a random graph with fixed connectivity $c = M + 1$. In the following, with a slight abuse of notation, we will also refer to this kind of graph as a Bethe lattice. The relevant iterative equation is [11]

$$P(u) = \int P_M(u_M) du_M \overline{\delta\left(u - \tilde{u}(J, u_M + H)\right)} \quad (6)$$

with the overline being the average with respect to the distribution of the quenched coupling J and

$$\tilde{u}(J, h) \equiv \frac{1}{\beta} \operatorname{arctanh}(\tanh \beta J \tanh \beta h). \quad (7)$$

The function P_M is the distribution of the sum of M independent fields, each one distributed according to P , i.e.,

$$P_K(u) = \int \prod_{i=1}^K P(u_i) du_i \delta\left(u - \sum_{i=1}^K u_i\right). \quad (8)$$

We will show that the dAT line, where by definition χ_{SG} diverges, is specified by the condition that the following homogeneous linear equation admits a non-zero solution $g(u)$:

$$g(u) = M \int du_M du_1 P_{M-1}(u_M - u_1) g(u_1) \overline{\delta\left(u - \tilde{u}(J, u_M + H)\right) \left(\frac{d\tilde{u}(J, u_M + H)}{dH}\right)^2} \quad (9)$$

where the derivative inside the integral reads

$$\frac{d\tilde{u}(J, h)}{dh} = \frac{[\tanh(\beta J) - \tanh(\beta h)]^2}{[1 - \tanh(\beta h)]^2 \tanh(\beta J)}. \quad (10)$$

Then we will show that the six-point susceptibilities needed to determine the parameter exponent at criticality can be expressed in terms of the eigenvector $g(u)$ of the integral equation (9). More precisely, one obtains

$$\frac{\omega_2}{\omega_1} = \frac{\langle\langle 2m_0^2(1 - m_0^2)^2 \rangle\rangle}{\langle\langle (1 - m_0^2)^3 \rangle\rangle} \quad (11)$$

where

$$m_0 = \tanh \beta [u_1 + u_2 + u_3 + u_{M-2} + H] \quad (12)$$

and

$$\langle\langle \dots \rangle\rangle \equiv \int du_1 du_2 du_3 du_{M-2} g(u_1)g(u_2)g(u_3)P_{M-2}(u_{M-2}) \dots \quad (13)$$

Note that since equation (9) is homogeneous the eigenvector $g(u)$ is specified up to a normalization constant but the ratio ω_2/ω_1 is independent of it.

As discussed in [3, 4], the connection between the parameter exponent λ and the ratio ω_2/ω_1 is rather general and holds not only for the SG transition in a field but also in the case of discontinuous SG transitions described dynamically by the mode-coupling-theory phenomenology. Furthermore, it has been shown that the ratio ω_2/ω_1 also plays a crucial role in off-equilibrium dynamics [8, 9]. In order to realize these different types of transitions one can consider, for instance, SG models with p -spin interactions or with Potts spins. Although in this paper we shall only consider the case of Ising spins with two-body interactions on fixed-connectivity graphs, we stress once again that analogous expressions can be obtained in more complex situations through straightforward extensions of the cavity arguments used in the following.

We note that the expression for the susceptibility can also be generalized. Indeed, the above equation for the critical condition is an instance of a sequence of eigenvalue equations of the general form

$$\mu_k g(u) = \int du_M du_1 P_{M-1}(u_M - u_1) g(u_1) \delta(u - \tilde{u}(J, u_M + H)) \left(\frac{d\tilde{u}(J, u_M + H)}{dH} \right)^k \quad (14)$$

that can be used in order to obtain higher order moments of the susceptibility; see [18] where this method has been applied in order to study the multi-fractal distribution of connected correlations at large distance.

3. The equation for the critical point

3.1. Derivation of the equation

A derivation of the condition (9) by means of the cavity method has been given in [13]. In this section we will present an alternative derivation which is the key to unveiling

the connection between the critical eigenvector and the computation of the six-point susceptibilities (which are also related to cubic cumulants of the order parameter). Our starting point is the spin-glass susceptibility which, due to the average over disorder, can be rewritten with respect to a given site s_0 of the Bethe lattice as

$$\chi_{\text{SG}} = \sum_i \overline{\langle s_0 s_i \rangle_c^2} = \sum_i \overline{\left(\frac{dm_0}{dH_i} \right)^2} \quad (15)$$

where m_0 is the magnetization of the root s_0 and H_i is a local field on site i . For a given site i we define its father $j = F(i)$ as the spin $j \in \partial 0$, with $\partial 0$ being the set of neighbors of 0, such that i is connected to 0 through j . On the other hand, the magnetization on the root can be written as

$$m_0 = \tanh \beta h_0, \quad h_0 = H_0 + \sum_{j \in \partial 0} u_{j \rightarrow 0} \quad (16)$$

where $u_{j \rightarrow 0}$ is by definition the field acting on site zero when all its neighbors except j are removed (in the language of computer science it would be the message passed from site j to site zero). Therefore, we have

$$\frac{dm_0}{dH_i} = (1 - m_0^2) \frac{du_{j \rightarrow 0}}{dH_i} \quad j = F(i). \quad (17)$$

Due to the locally tree-like nature of the lattice, the field $u_{j \rightarrow 0}$ is influenced only by a field on one of its sons $i \in S(j)$, defined such that $j = F(i)$; therefore, we may write

$$\sum_i \left(\frac{dm_0}{dH_i} \right)^2 = (1 - m_0^2)^2 \left[1 + \sum_{j \in \partial 0} \sum_{k \in S(j)} \left(\frac{du_{j \rightarrow 0}}{dH_k} \right)^2 \right] \quad (18)$$

where in the above expression the 1 is present in order to take into account the case in which the site i is the root itself. At this point we introduce the following physical object in order to average over the disorder:

$$\chi(u) \equiv \overline{\delta(u - u_{j \rightarrow 0}) \sum_{k \in S(j)} \left(\frac{du_{j \rightarrow 0}}{dH_k} \right)^2}. \quad (19)$$

In principle, we should have written $\chi_j(u)$, but the difference between different branches has disappeared due to the disorder average. In physical terms $\chi(u)$ is essentially the spin-glass susceptibility of a given branch conditioned to the fact that the value of the field $u_{j \rightarrow 0}$ is u . Indeed, using equation (18) we can see that the total χ_{SG} can now be written as an integral of $\chi(u)$ over possible values of u ,

$$\begin{aligned} \chi_{\text{SG}} &= \int P_{M+1}(u) [1 - \tanh^2(\beta H + \beta u)]^2 du \\ &\quad + (M + 1) \int P_M(u') \chi(u'') [1 - \tanh^2(\beta H + \beta(u' + u''))]^2 du' du''. \end{aligned} \quad (20)$$

Performing essentially the same steps as for the total χ_{SG} one can obtain the following iterative equation for the function $\chi(u)$:

$$\begin{aligned} \chi(u) = & \int P_M(u') \delta[u - \tilde{u}(J, u' + H)] \left(\frac{d\tilde{u}(J, u' + H)}{dH} \right)^2 du' \\ & + M \int P_{M-1}(u') \chi(u'') \\ & \times \delta[u - \tilde{u}(J, u' + u'' + H)] \left(\frac{d\tilde{u}(J, u' + u'' + H)}{dH} \right)^2 du' du'' \end{aligned} \quad (21)$$

where we have used the definitions of section 2. Note that we need the whole function $\chi(u)$ in order to write the iterative equation and this why we introduced it in the first place. The above equation can be solved, leading to a finite $\chi(u)$ and χ_{SG} , provided that the linear system is invertible. This is not possible, meaning that we are at a critical point, if the corresponding homogeneous linear system, i.e. equation (9), admits a non-zero solution, thus completing our argument. The function $\chi(u)$ diverges at the critical point and standard arguments tell us that the critical eigenvector $g(u)$ controls its divergence. More precisely we have

$$\chi(u) \propto \frac{g(u)}{\tau} \quad (22)$$

where τ depends on the external parameters (e.g. temperature and field) and vanishes linearly at the critical point.

3.2. Solving the critical equation

Now we want to show how to actually solve equation (9) and to connect it to the original method for computing the dAT line. The standard way to compute $P(u)$ from equation (6) is by population dynamics: the function $P(u)$ is approximated by a population of N fields, $P(u) = N^{-1} \sum_{i=1}^N \delta(u - u_i)$, which plugged into the rhs produces a new sum of delta functions, which is a new population. On iterating this process several times the population may converge to a good approximation for the $P(u)$ that solves the self-consistency equation (6).

The computation of $g(u)$ from equation (9) is not straightforward. Indeed, if both $P(u)$ and $g(u)$ are approximated by populations, then the rhs of equation (9) would result in a *weighted* population, due to the extra factor

$$f(\beta J, \beta u) = \left(\frac{[\tanh(\beta J) - \tanh(\beta u)]^2}{[1 - \tanh(\beta u)]^2 \tanh(\beta J)} \right)^2.$$

Working with a weighted population is not a good idea, because if the weights become very different, then the effective size of the population gets reduced. Just to illustrate the concept with an extremal case, if half of the population elements get a null weight the effective size of the population gets reduced by at least a factor of 2.

The problem of solving a self-consistent integral equation containing a reweighting term $f(\beta J, \beta u)$ is not new, as it appears, e.g., in 1RSB equations obtained by the replica

method [16] or the cavity method [11] and even in more complicated equation obtained by the replica cluster variational method [17].

A possible way to solve these equation is that of discretizing the $g(u)$ by approximating it with a histogram of N bins. The fact that equation (3) is linear in $g(u)$ implies that the equations for the N heights of the histogram bins are again linear. In practice, one should compute the largest eigenvalue of a random $N \times N$ matrix that depends on the fixed point $P(u)$ (which can be kept as a population); when this eigenvalue equals 1 then equation (9) is satisfied and the system is at the critical point.

We prefer to approximate $g(u)$ by a population (as we always do for $P(u)$ as well) and we devise two different methods for solving equation (9).

In the first method, the factor $f(\beta J, \beta u)$ is interpreted as the probability that the newly generated element should be included in the new population representing $g(u)$. In the present case we have that $0 \leq f(\beta J, \beta u) \leq 1$ and so the interpretation as a probability is straightforward. In more complicated cases [18], the reweighting factor may be larger than 1 and in that case more than one copy of the same new element should be eventually included in the new population. If this is the case, we suggest that the new population should be made larger than the old one, and then it should be filtered by randomly choosing its elements; in this way a much smaller fraction of twin elements will finally remain in the new population and the information content of the population is preserved.

The second method is essentially equivalent to the original method invented to identify the location of the dAT line in sparse models [19]. Each cavity field u_i is perturbed by an infinitesimal quantity δu_i and the evolution of the pairs $(u_i, \delta u_i)$ is followed according to the belief propagation (BP) equations. Thanks to the symmetry of the interactions, we have that $\langle \delta u_i | u_i = u \rangle = 0$ for any u value and the interesting quantities to look at are the variances, which evolve under BP by the following equation:

$$\langle \delta u^2 | u \rangle_{t+1} = M \int du_1 \langle \delta u^2 | u_1 \rangle_t \times \prod_{i=2}^M dP(u_i) \delta \left(u - \tilde{u} \left(J, H + \sum_{i=1}^M u_i \right) \right) \left(\frac{[\tanh(\beta J) - \tanh(\beta u)]^2}{[1 - \tanh(\beta u)]^2 \tanh(\beta J)} \right)^2 \quad (23)$$

which corresponds to equation (9) by equating $g(u) = \langle \delta u_i^2 | u_i = u \rangle$ in the large time limit. Equation (23) has a non-zero solution only at the critical point. Therefore, in order to measure $g(u) = \langle \delta u^2 | u \rangle$ also away from the critical point one can renormalize it at each BP step, and this corresponds to solving the following equation:

$$g(u) = \mu M \int du_1 g(u_1) \times \prod_{i=2}^M dP(u_i) \delta \left(u - \tilde{u} \left(J, H + \sum_{i=1}^M u_i \right) \right) \left(\frac{[\tanh(\beta J) - \tanh(\beta u)]^2}{[1 - \tanh(\beta u)]^2 \tanh(\beta J)} \right)^2 \quad (24)$$

where μ is the inverse of the normalization factor in the large time limit. The above equation no longer depends on time, but only involves asymptotic quantities and the new parameter μ . It admits a non-zero solution at any temperature and external field. Interpretation of equation (24) is straightforward: in the high temperature paramagnetic

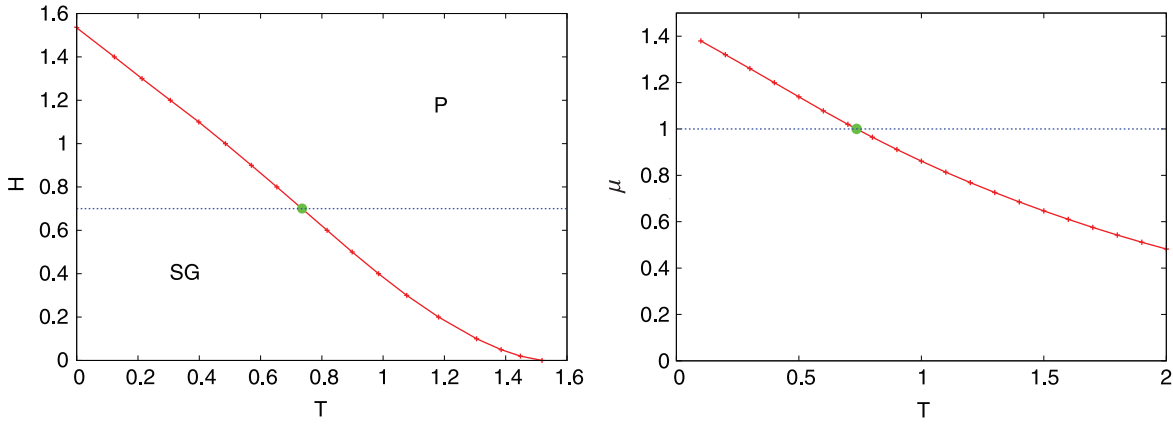


Figure 1. Left panel: critical dAT line for a spin-glass model with couplings $J_{ij} = \pm 1$ and external field h on a random regular graph (Bethe lattice) of fixed degree $M + 1 = 4$. Right panel: maximum eigenvalue μ of the integral kernel in equation (24) computed along the blue line in the left panel ($H = 0.7$).

phase $\mu < 1$, so any perturbation goes to zero exponentially as μ^t and the BP fixed point is stable; in the low temperature spin-glass phase $\mu > 1$, a perturbation grows as μ^t and the BP fixed point is unstable (indeed the correct solution is provided by an Ansatz breaking the replica symmetry).

In practice, after having computed the $P(u)$ from equation (6) by population dynamics, we solve equation (24), by one of the two methods described above, and we compute the maximum eigenvalue μ of the integral kernel and the corresponding eigenvector $g(u)$.

We present data obtained for a spin-glass model ($J_{ij} = \pm 1$ with equal probabilities and uniform external field h) on a random regular graph (Bethe lattice) with fixed degree $M + 1 = 4$. The dAT line for this model was already presented in [20] and is reproduced in figure 1 (left panel) for completeness. In figure 1 (right panel) we show the maximum eigenvalue μ as a function of the temperature at a fixed field $H = 0.7$ (horizontal line in the left panel); the behavior is exactly that discussed above.

In figure 2 (upper panel) we show the fixed point distribution of cavity fields, $P(u)$, at several temperatures and fixed external field $H = 0.7$ (please note that the y axis is in log scale). It is worth noticing that the $P(u)$ becomes broader by lowering the temperature, but has no particular change at the critical temperature, $T_c(H = 0.7) = 0.7353$, and finally becomes singular at zero temperature (we comment more on this below). In figure 2 (lower panel) we show the eigenfunction $g(u)$ corresponding to the maximum eigenvalue μ . It is worth noticing that these functions are even smoother than the corresponding $P(u)$ and even in the $T = 0$ limit $g(u)$ remains continuous, although with steps (further comments are given below).

The method presented in this paper is perfectly suitable for the study of critical properties of disordered models defined on random graphs. Indeed, the functions $P(u)$ and $g(u)$ are well defined on the entire critical line and smooth enough (infinitely differentiable) for any $T > 0$. Even at $T = 0$ they are well defined distributions, which lead to smooth physical observables, once integrated over.

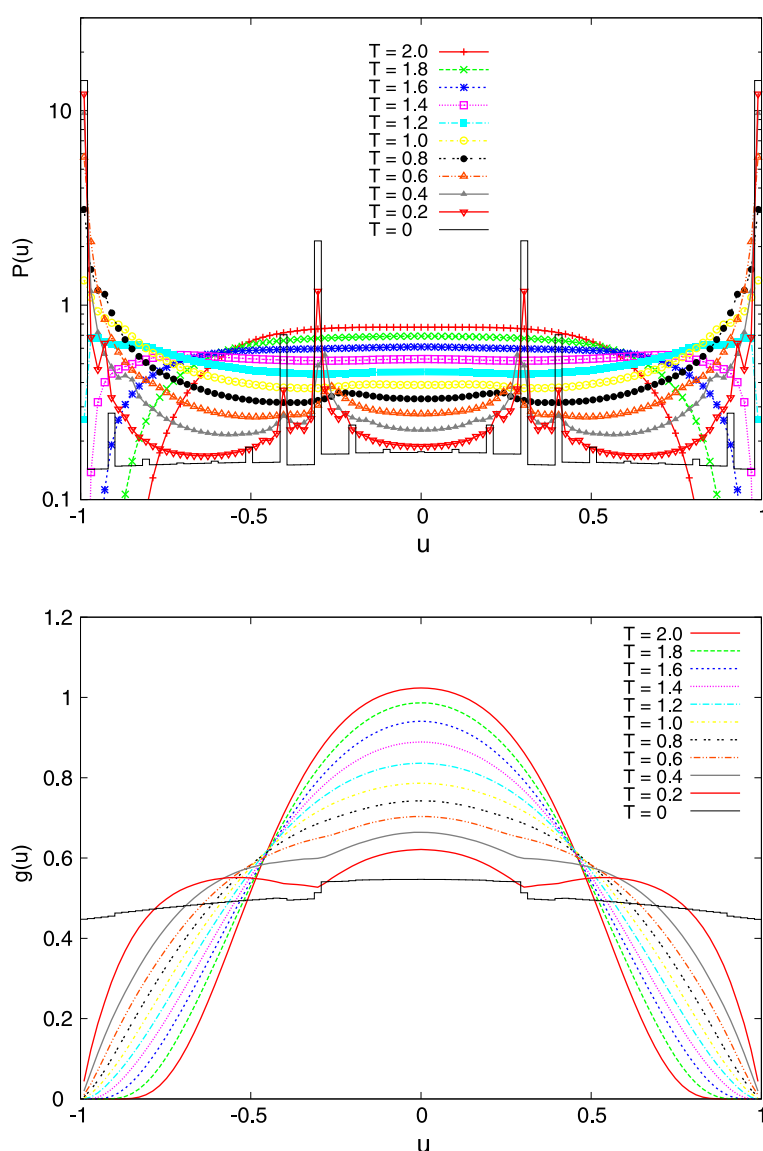


Figure 2. Fixed point $P(u)$ (upper panel) and $g(u)$ (lower panel) for $H = 0.7$ and several temperatures (including $T = 0$).

In figure 3 we show these functions computed at several points along the critical line, including the $T = 0$ critical point for $g(u)$. Actually, in the lower panel of figure 3 we have included three different $g(u)$ s computed at $T = 0$ with field values which are all compatible with our best estimate for the critical field, $H_c = 1.534(1)$. The comparison of these three distributions should make the reader aware of which features of the critical $g(u)$ at $T = 0$ are robust with respect to very small field fluctuations and which are not.

Once we have the process for computing the critical distributions $P(u)$ and $g(u)$ along the entire critical line under control, we can use the resulting data to estimate universal quantities of physical interest.

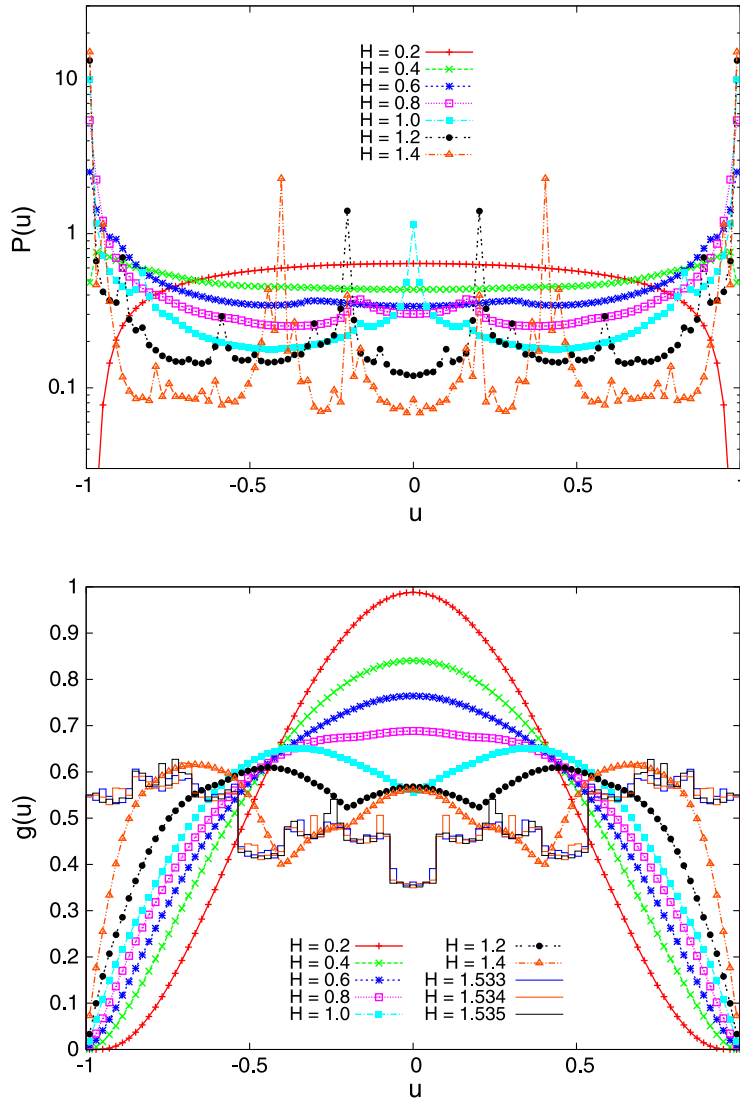


Figure 3. Fixed point $P(u)$ (upper panel) and $g(u)$ (lower panel) for several points along the critical dAT line, indexed by the corresponding field value. The lower panel also shows the $g(u)$ computed at $T = 0$ with three field values, all compatible with our best estimate for $H_c = 1.534(1)$.

3.3. The zero temperature limit

The computation of the functions $P(u)$ and $g(u)$ at $T = 0$ requires some more care, because these functions may develop singularities. The BP equation to be satisfied by the cavity field population $P(u)$ is the following:

$$P(u) = \int \prod_{i=1}^M P(u_i) \overline{\delta\left(u - \hat{u}_J\left(H + \sum_i u_i\right)\right)} \quad (25)$$

with $\hat{u}_J(x) = \text{sign}(Jx) \min(|x|, 1)$, where we have assumed $|J| = 1$ without loss of generality. The function \hat{u} essentially moves the weight of fields such that $|H + \sum_i u_i| > 1$

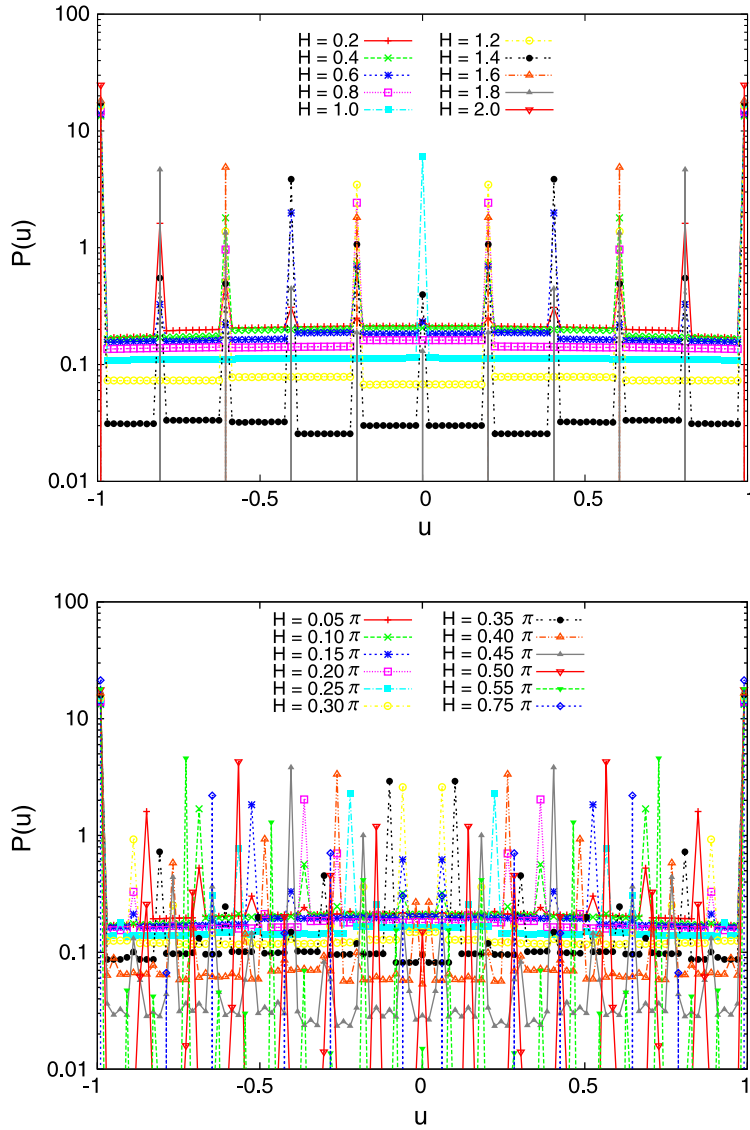


Figure 4. Fixed point $P(u)$ for $T = 0$ and several external fields.

on the extrema of the allowed domain $u \in [-1, 1]$. Therefore, the fixed point function $P(u)$ is a distribution with at least two delta functions in $u = 1$ and -1 . Depending on the value of the external field H , further delta peaks are present in $P(u)$ at values $u = n|J| + mH$ with integer valued n and m .

In figure 4 (upper panel) we show distributions $P(u)$ computed at $T = 0$ with H being a multiple of $\Delta = 0.2$, and the presence of peaks equally spaced by Δ is evident. Such a regularity in peak location is present only if the external field and the coupling interaction can be written as $H = n_1\Delta$ and $|J| = n_2\Delta$, with integer valued n_1 and n_2 , and Δ being the peak distance. For example, in figure 4 (lower panel) we show distributions $P(u)$ computed with an external field that does not satisfy the above requirement, and indeed the peaks have less regular positions.

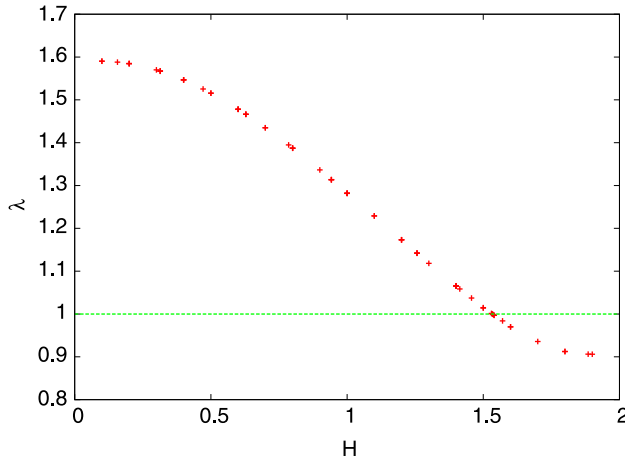


Figure 5. Maximum eigenvalue μ of the $T = 0$ integral kernel in equation (26) as a function of the external field H .

What is more interesting to notice is the continuous part between the peaks; this ‘background’ only exists in the low temperature spin-glass phase where the replica symmetry should be broken, as was already noticed in [21]. The reason for this is simple: in the paramagnetic phase (where the RS solution is exact) the distribution $P(u)$ made of Δ -spaced delta peaks solves the BP equations and is stable with respect to small perturbations. What was less obvious is that starting from a generic initial condition (e.g., we start with a distribution uniform in $[-1, 1]$) the population dynamics algorithm always converges to this solution in the paramagnetic phase. In the spin-glass phase the presence of the continuous part in $P(u)$ is due to the instability of the Dirac deltas with respect to any perturbation; the only compromise is the coexistence of these delta peaks with a continuous part. We have checked that, as expected, the weight of the continuous part goes to zero at the critical point, which can be easily identified by study of the largest eigenvalues μ of the following linear integral equation:

$$g(u) = \mu M \int P_{M-1}(u_M - u_1) g(u_1) du_M du_1 \overline{\delta(u - (u_M + H)\text{sign } J) \theta(|J| - |u_M + H|)}. \quad (26)$$

The largest eigenvalue μ computed at $T = 0$ as a function of the external field is shown in figure 5 and provides the following estimate for the critical field: $H_c(T = 0) = 1.534(1)$.

At $T = 0$ the eigenvector $g(u)$ presents Heaviside steps where the corresponding $P(u)$ has Dirac deltas. We show in figure 6 the distributions $g(u)$ computed at the same field values as in figure 4. In general, the distribution $g(u)$ is less singular than the corresponding $P(u)$. We observed that $g(u)$ becomes more singular on approaching the zero temperature critical point (see figure 3 and related comments below).

It is interesting to consider the large M limit of the dAT line. At finite temperature one expects to obtain the standard dAT line of the Sherrington–Kirkpatrick model. However, while the dAT line of the SK model has $H_{\text{dAT}}(0) = \infty$ at zero temperature, in diluted models $H_{\text{dAT}}(0)$ is finite at any finite value of M that diverges in the large M limit. In

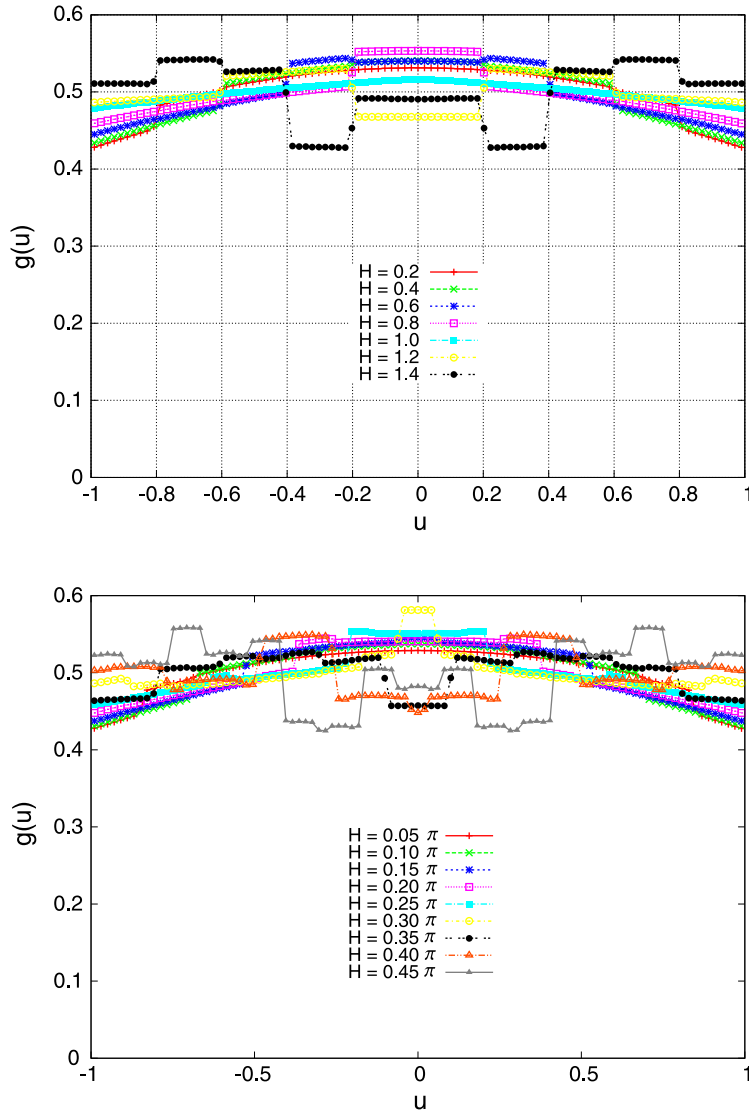


Figure 6. Fixed point $g(u)$ for $T = 0$ and several external fields.

order to characterize this behavior we will have to first take the $\beta \rightarrow \infty$ limit and then the $M \rightarrow \infty$ limit. The final result, derived in the appendix, is

$$\frac{1}{M^{1/2}} \simeq \frac{2\sqrt{|J|}}{\sqrt{2\pi J^2}} \exp\left[-\frac{H_{\text{dAT}}^2}{2J^2}\right]. \quad (27)$$

Therefore, H_{dAT} diverges with M as $H_{\text{dAT}} = \sqrt{J^2 \ln M}$.

4. Six-point susceptibilities at criticality

In this section we will derive expressions for the two six-point susceptibilities ω_1 and ω_2 , whose ratio is directly related to the dynamical exponents according to equation (3). We

start with the computation of ω_1 , whose definition is

$$\omega_1 = \frac{1}{N} \sum_{ijk} \overline{\langle s_i s_j \rangle_c \langle s_j s_k \rangle_c \langle s_k s_i \rangle_c}. \quad (28)$$

We will see that ω_1 diverges at criticality as τ^{-3} where τ is the same as in equation (22). In order to compute $\overline{\langle s_i s_j \rangle_c \langle s_j s_k \rangle_c \langle s_k s_i \rangle_c}$ we will consider only the case in which the three indices are different. Indeed, one can check at the end that this is the only relevant case at criticality, because the remaining two cases give contributions that either are not diverging or are diverging with a power less than τ^{-3} .

Let us label the spins s_1 , s_2 and s_3 , and let us denote by s_0 the spin where the three paths on the tree that connects the spins s_1 , s_2 and s_3 join. This does not include the case in which, say, spin s_1 lies on the line connecting spins s_2 and s_3 , but it can also be argued that this gives a less divergent contribution and can be neglected at the critical point. We also denote by $s_{1'}$, $s_{2'}$ and $s_{3'}$ the neighbors of s_0 on the branches where s_1 , s_2 and s_3 respectively lie. Now let us consider the connected correlation

$$\langle s_1 s_2 \rangle_c = \frac{1}{\beta} \frac{dm_2}{dH_1}. \quad (29)$$

Given the locally tree-like nature of the graph the response of m_2 would be the same in the presence of an external field on site s_0 proportional to the derivative of the field passed from $s_{1'}$ to s_0 ,

$$\frac{dm_2}{dH_1} \equiv \frac{dm_2}{dH_0} \frac{du_{1' \rightarrow 0}}{dH_1}. \quad (30)$$

On the other hand, we have

$$\frac{dm_2}{dH_0} = \frac{dm_0}{dH_2} = \frac{dm_0}{dH_0} \frac{du_{2' \rightarrow 0}}{dH_2} = \beta(1 - m_0^2) \frac{du_{2' \rightarrow 0}}{dH_2} \quad (31)$$

where m_0 is the magnetization of site s_0 induced by the global cavity field acting on it,

$$m_0 = \tanh \beta H_0; \quad H_0 = \sum_{i \in \partial 0} u_{i \rightarrow 0}. \quad (32)$$

Putting everything together, we arrive at the following useful relationship:

$$\langle s_1 s_2 \rangle_c = (1 - m_0^2) \frac{du_{2' \rightarrow 0}}{dH_2} \frac{du_{1' \rightarrow 0}}{dH_1}. \quad (33)$$

Using the above relationship for $\langle s_1 s_3 \rangle_c$ and $\langle s_2 s_3 \rangle_c$ we finally obtain

$$\langle s_1 s_2 \rangle_c \langle s_2 s_3 \rangle_c \langle s_3 s_1 \rangle_c = (1 - m_0^2)^3 \left(\frac{du_{2' \rightarrow 0}}{dH_2} \right)^2 \left(\frac{du_{1' \rightarrow 0}}{dH_1} \right)^2 \left(\frac{du_{3' \rightarrow 0}}{dH_3} \right)^2. \quad (34)$$

In the next step we have to average the above expression over the disorder and the positions of sites s_1 , s_2 and s_3 and the N possible values of the central spin s_0 . It is clear that the three terms $du_{1' \rightarrow 0}/dH_1$, $du_{2' \rightarrow 0}/dH_2$ and $du_{3' \rightarrow 0}/dH_3$ are uncorrelated between each other; however, they are correlated with the corresponding messages $u_{1' \rightarrow 0}$, $u_{2' \rightarrow 0}$ and

$u_{3' \rightarrow 0}$. Therefore, we can perform the integration over them with the help of the function $\chi(u)$ defined in equation (19). In the end we arrive at the following expression:

$$\frac{1}{N} \sum_{i \neq j \neq k} \overline{\langle s_i s_j \rangle_c \langle s_j s_k \rangle_c \langle s_k s_i \rangle_c} = \binom{M+1}{3} \int du_1 du_2 du_3 du_{M-2} \times \chi(u_1) \chi(u_2) \chi(u_3) P_{M-2}(u_{M-2}) (1 - m_0^2)^3 + o(\tau^{-3}) \quad (35)$$

where

$$m_0 = \tanh \beta [u_1 + u_2 + u_3 + u_{M-2} + H] \quad (36)$$

and $P_{M-2}(u_{M-2})$ is the distribution of the sum of $M - 2$ fields distributed independently according to the function $P(u)$. According to equation (22), at criticality the joint susceptibility $\chi(u)$ diverges and can be written as a solution $g(u)$ of the homogeneous equation (9) times a constant diverging as the inverse of the distance from the critical point τ . Then, it follows that ω_1 diverges as τ^{-3} . We stress that the above expression is only valid at leading order and we can now show that the cases we did not consider give contributions that are less divergent at criticality. It is immediate to verify that the case in which the three spins are equal gives a contribution that remains finite at criticality. The case in which only two spins are equal can be obtained following the derivation of section 3, assuming that the two coinciding spins are located on the root; the final result is

$$\frac{1}{N} \sum_{i \neq j} \overline{\langle s_i s_j \rangle_c^2 (1 - \langle s_i \rangle^2)} = (M+1) \int P_M(u') \chi(u'') [1 - \tanh^2(\beta H + \beta(u' + u''))]^3 du' du''. \quad (37)$$

From this we see immediately that this quantity diverges only as τ^{-1} at criticality. Finally, the case in which the three spins are different but are arranged on a single path is equivalent in the above framework to the assumption that one of the three spins coincides with s_0 , and it is straightforward to verify that this gives a contribution diverging as τ^{-2} .

Now we turn to the computation of the second cumulant

$$\omega_2 = \frac{1}{2N} \sum_{ijk} \overline{\langle s_i s_j s_k \rangle_c^2}. \quad (38)$$

We proceed as above and we write

$$\langle s_1 s_2 s_3 \rangle_c = \frac{1}{\beta^2} \frac{dm_2}{dH_1 dH_3}. \quad (39)$$

This can be obtained by deriving equation (33) with respect to H_3 . It is evident that the only term that depends on H_3 is the field $u_{3' \rightarrow 0}$ entering in the expression of m_0 ; therefore, we can write

$$\langle s_1 s_2 s_3 \rangle_c = 2m_0 (1 - m_0^2) \frac{du_{1' \rightarrow 0}}{dH_1} \frac{du_{2' \rightarrow 0}}{dH_2} \frac{du_{3' \rightarrow 0}}{dH_3}. \quad (40)$$

Squaring the above expression and proceeding as above we can write:

$$\frac{1}{2N} \sum_{i \neq j \neq k} \overline{\langle s_i s_j s_k \rangle_c^2} = \binom{M+1}{3} \int du_1 du_2 du_3 du_{M-2} \chi(u_1) \chi(u_2) \chi(u_3) P_{M-2}(u_{M-2}) \times 2m_0^2(1-m_0^2)^2 + o(\tau^{-3}). \quad (41)$$

The first term corresponds to the assumption that the three spins are different and are connected through a spin s_0 different from each of them. We can easily repeat the analysis for ω_1 and show that this term gives a contribution diverging as τ^{-3} at criticality while the other terms in (38) give less divergent contributions.

Since in the critical region $\chi(u)$ is proportional to $g(u)$ according to equation (22) we can now express the coefficient ω_2/ω_1 as

$$\frac{\omega_2}{\omega_1} = \frac{\langle\langle 2m_0^2(1-m_0^2)^2 \rangle\rangle}{\langle\langle (1-m_0^2)^3 \rangle\rangle} \quad (42)$$

where

$$m_0 = \tanh \beta[u_1 + u_2 + u_3 + u_{M-2} + H] \quad (43)$$

and

$$\langle\langle \cdots \rangle\rangle = \int du_1 du_2 du_3 du_{M-2} g(u_1)g(u_2)g(u_3)P_{M-2}(u_{M-2}) \cdots \quad (44)$$

This completes the derivation of equation (11). We note that in the large M limit one can easily check that the above expression reduces to the results of Sompolinsky and Zippelius for the SK model; see equations (6.20) and (6.21) in [22].

It is also interesting to consider the zero temperature limit of the ratio ω_2/ω_1 . In order to do so we have to consider the distribution of the variable $u_0 = u_1 + u_2 + u_3 + u_{M-2} + H$ in (43). If this variable has a continuous distribution $P_0(u_0)$ in the $T \rightarrow 0$ limit we can make the rescaling $\beta u_0 = y$ in (42). Now the region relevant for the integrals is the region corresponding to $u_0 = 0$ where $P_0(u_0)$ can be replaced by $P(0)$; the net result is

$$\frac{\omega_2}{\omega_1} = \frac{\int_{-\infty}^{\infty} 2 \tanh^2 y (1 - \tanh^2 y)^2 dy}{\int_{-\infty}^{\infty} (1 - \tanh^2 y)^3 dy} = \frac{1}{2}. \quad (45)$$

Note that this result holds independently of the connectivity and it also coincides with the result for the SK model in the $T \rightarrow 0$ limit.

In figure 7 we plot the ratio ω_2/ω_1 computed according to the formula (42) on the dAT line of the Bethe lattice model with connectivity $M+1=4$. The data shown satisfy the expected zero temperature limit $\omega_2/\omega_1 = 1/2$. The ratio increases from zero to $1/2$ upon lowering the temperature and correspondingly the dynamical exponent a defined by equation (3) decreases from $1/2$ to 0.395 . The value of $a = 0.404$ that can be read for $H = 0.7$ was compared in previous work with numerical data, displaying a very good agreement; see figure 1 in [4].

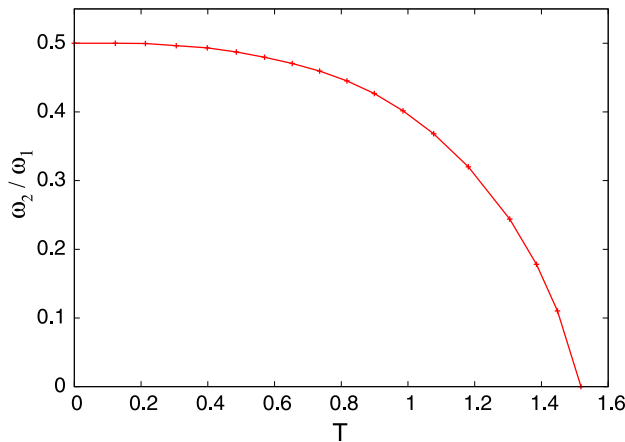


Figure 7. The ratio ω_2/ω_1 computed along the critical dAT line as a function of the temperature for the Bethe lattice SG with connectivity $c = 4$. The ratio tends to $1/2$ at zero temperature.

5. Conclusions

We have presented a method, based on cavity arguments, to compute the spin-glass and higher order susceptibilities in diluted mean-field spin-glass models. The divergence of the spin-glass susceptibility is associated with the existence of a non-zero solution of a homogeneous linear integral equation. Six-point susceptibilities, relevant for the $q(x)$ function in the RSB phase and for critical dynamics through the parameter exponent λ , can be expressed at criticality as integrals involving the critical eigenvector. The numerical evaluation of the corresponding analytic expressions down to zero temperature has been discussed together with the connection with alternative numerical methods. The method was illustrated in the context of the de Almeida–Thouless line for a spin glass on a Bethe lattice but can be generalized straightforwardly to more complex situations. The key for the derivation is equation (33), from which one can express the six-point susceptibilities in terms of the joint susceptibility $\chi(u)$, which is in turn proportional to the eigenvector $g(u)$ of the homogeneous integral equation at criticality. We note that in the case of factor graphs, corresponding to p -spin interactions, one has to take into account that the node connecting the three spins in the discussion of section 4 can be either a factor or a variable node, but it is straightforward to derive the equivalent of equation (33) for a factor node.

Acknowledgments

This research has received financial support from the European Research Council (ERC) through grant agreement No. 247328 and from the Italian Research Minister through the FIRB project No. RBFR086NN1.

Appendix. The SK limit at finite and zero temperature

In this appendix we study the dAT line analytically in the large- M limit. *At any finite temperature* we will recover the standard dAT line of the Sherrington–Kirkpatrick model.

It is well known that the dAT line of the SK model has $H_{\text{dAT}}(0) = \infty$ at zero temperature; instead in diluted models $H_{\text{dAT}}(0)$ is finite at any finite value of M but diverges in the large M limit. In order to characterize this behavior we will have to first take the $\beta \rightarrow \infty$ limit and then the $M \rightarrow \infty$ limit.

In order to reach the large- M limit we must consider rescaled couplings $J/M^{1/2}$ with J finite. As a consequence, the distribution $P_M(u_M)$ becomes a Gaussian with a finite variance. The distribution $P(u)$ instead is concentrated on very small values of u and it is appropriate to consider the distribution of the variable $y = uM^{1/2}$. The distribution of y is given according to equation (6) by

$$P(y) = \int P_M(u_M) du_M \delta \left(y - \frac{M^{1/2}}{\beta} \operatorname{arctanh} \left[\tanh \frac{\beta J}{M^{1/2}} \tanh[\beta u_M + \beta H] \right] \right). \quad (\text{A.1})$$

In the large M limit we have

$$\frac{M^{1/2}}{\beta} \operatorname{arctanh} \left[\tanh \frac{\beta J}{M^{1/2}} \tanh[\beta u_M + \beta H] \right] \rightarrow J \tanh[\beta u_M + \beta H]. \quad (\text{A.2})$$

The function $P_M(u_M)$ according to equation (8) becomes a Gaussian in the large- M limit with a variance equal to the variance of y ; this leads to the standard replica symmetric equation of the SK model

$$q = \int P(z) \tanh[\beta z + \beta H]^2 dz, \quad P(z) = \frac{1}{\sqrt{2\pi q J^2}} \exp \left[-\frac{z^2}{2q J^2} \right]. \quad (\text{A.3})$$

In order to write the dAT condition (9) in the SK limit we note that the function $g(u)$ is also concentrated around small values of u and can be approximated with a delta function on the rhs of equation (9). Integrating equation (9) in u one obtains the following homogeneous equation for $g \equiv \int g(u) du$:

$$g = M \int P(z) dz \left(\frac{\sinh[2\beta J/M^{1/2}]}{\cosh[2\beta J/M^{1/2}] + \cosh[2\beta(z + H)]} \right)^2 g \quad (\text{A.4})$$

where we have used the following alternative representation of $d\tilde{u}/dh$:

$$\frac{[\tanh(\beta J) - \tanh(\beta h)]^2}{[1 - \tanh(\beta h)]^2 \tanh(\beta J)} = \frac{\sinh[2\beta J]}{\cosh[2\beta J] + \cosh[2\beta h]}. \quad (\text{A.5})$$

In the large- M limit we have

$$\lim_{M \rightarrow \infty} M \left(\frac{\sinh[2\beta J/M^{1/2}]}{\cosh[2\beta J/M^{1/2}] + \cosh[2\beta(z + H)]} \right)^2 = J^2 \beta^2 (1 - \tanh^2[\beta(z + H)])^2 \quad (\text{A.6})$$

thus, we recover the dAT line for the SK model

$$1 = \int P(z) dz \bar{J}^2 \beta^2 (1 - \tanh^2[\beta(z + H)])^2. \quad (\text{A.7})$$

The zero temperature limit of this equation can be obtained by noticing that the variance of the Gaussian distribution $P(z)$ goes to $\overline{J^2}$ and that

$$\lim_{\beta \rightarrow \infty} \beta(1 - \tanh^2[\beta z])^2 = \frac{4}{3} \delta(z). \quad (\text{A.8})$$

This leads to

$$T \simeq \frac{4 \overline{J^2}^{1/2}}{3\sqrt{2\pi}} \exp\left[-\frac{H^2}{2\overline{J^2}}\right]. \quad (\text{A.9})$$

As a consequence, $H_{\text{dAT}}(T)$ goes to infinity at low temperatures. On the other hand, it must remain finite at any finite M , and in order to get its behavior we must take the large β limit before the large M limit. In this case we can proceed as before in order to get to equation (A.4). However, in the next equation we have to take $\beta \rightarrow \infty$ first, and due to its non-linearity this gives

$$\lim_{\beta \rightarrow \infty} M \left(\frac{\sinh[2\beta J/M^{1/2}]}{\cosh[2\beta J/M^{1/2}] + \cosh[2\beta(z+H)]} \right)^2 = M\theta\left(\frac{|J|}{M^{1/2}} - |z+H|\right) \quad (\text{A.10})$$

where $\theta(z)$ is the step function. Taking $M \rightarrow \infty$ in the above equation we obtain

$$\lim_{M \rightarrow \infty} M\theta\left(\frac{|J|}{M^{1/2}} - |z|\right) \approx 2|J|M^{1/2}\delta(z). \quad (\text{A.11})$$

Substituting back into equation (A.4) we obtain the dAT equation in the large- M limit,

$$\frac{1}{M^{1/2}} \simeq \frac{2\overline{|J|}}{\sqrt{2\pi\overline{J^2}}} \exp\left[-\frac{H^2}{2\overline{J^2}}\right]. \quad (\text{A.12})$$

Therefore, H_{dAT} diverges with M as $H_{\text{dAT}} = \sqrt{\overline{J^2} \ln M}$. One may question the validity of the above result, noticing that we used the Gaussian approximation for the function $P_M(u_M)$ while (i) H is diverging with M (although logarithmically) and (ii) according to equation (A.10) we are basically integrating it on a region of size $M^{-1/2}$ where the function does not look at all like a Gaussian (consider, for instance, the case $J = \pm 1$). The result, however, is actually correct, as can be seen by means of a more precise analysis including corrections that we do not report for reasons of space. Such a computation can be performed considering the large M limit of equation (26) and rewriting the integral on the rhs by means of a Fourier transform.

References

- [1] Mézard M, Parisi G and Virasoro MA, 1987 *Spin Glass Theory and Beyond* (Singapore: World Scientific)
- [2] Gross D J, Kanter I and Sompolinsky H, 1985 *Phys. Rev. Lett.* **55** 304
- [3] Parisi G and Rizzo T, 2013 *Phys. Rev. E* **87** 012101
- [4] Caltagirone F, Ferrari U, Leuzzi L, Parisi G, Ricci-Tersenghi F and Rizzo T, 2012 *Phys. Rev. Lett.* **108** 085702
- [5] Caltagirone F, Parisi G and Rizzo T, 2012 *Phys. Rev. E* **85** 051504
- [6] Ferrari U, Leuzzi L, Parisi G and Rizzo T, 2012 *Phys. Rev. B* **86** 014204
- [7] Caltagirone F, Ferrari U, Leuzzi L, Parisi G and Rizzo T, 2012 *Phys. Rev. B* **86** 064204

- [8] Caltagirone F, Parisi G and Rizzo T, 2013 *Phys. Rev. E* **87** 032134
- [9] Rizzo T, 2013 *Phys. Rev. E* **88** 032135
- [10] De Dominicis C and Goldschmidt Y Y, 1989 *J. Phys. A: Math. Gen.* **22** L775
De Dominicis C and Goldschmidt Y Y, 1990 *Phys. Rev. B* **41** 2184
- [11] Mézard M and Parisi G, 2001 *Eur. Phys. J. B* **20** 217
- [12] Weigt M and Monasson R, 1996 *Europhys. Lett.* **36** 209
- [13] Janzen K, Engel A and Mézard M, 2010 *Phys. Rev. E* **82** 021127
- [14] Janzen K and Engel A, 2010 *J. Stat. Mech.* P12002
- [15] Parisi G and Rizzo T, 2005 *Phys. Rev. B* **72** 184431
- [16] Franz S, Leone M, Ricci-Tersenghi F and Zecchina R, 2001 *Phys. Rev. Lett.* **87** 127209
- [17] Rizzo T, Lage-Castellanos A, Mulet R and Ricci-Tersenghi F, 2010 *J. Stat. Phys.* **139** 375
- [18] Morone F, Parisi G and Ricci-Tersenghi F, 2013 arXiv:1308.2037
- [19] Pagnani A, Parisi G and Ratiéville M, 2003 *Phys. Rev. E* **68** 046706
- [20] Parisi G and Ricci-Tersenghi F, 2012 *Phil. Mag.* **92** 341
- [21] Montanari A, Parisi G and Ricci-Tersenghi F, 2004 *J. Phys. A: Math. Gen.* **37** 2073
- [22] Sompolinsky H and Zippelius A, 1982 *Phys. Rev. B* **25** 6860